Published in final edited form as:
Neurogastroenterol Motil. 2014 December ; 26(12): 1717–1729. doi:10.1111/nmo.12452.

Gastric vagal motoneuron function is maintained following experimental spinal cord injury

Emily M. Swartz and **Gregory M. Holmes***
Department of Neural and Behavioral Sciences, Penn State University College of Medicine Hershey, PA 17033

Abstract

Background: Clinical reports indicate that spinal cord injury (SCI) initiates profound gastric dysfunction. Gastric reflexes involve stimulation of sensory vagal fibers, which engage brainstem circuits that modulate efferent output back to the stomach, thereby completing the vago-vagal reflex. Our recent studies in a rodent model of experimental high thoracic (T3-) SCI suggest that reduced vagal afferent sensitivity to gastrointestinal (GI) stimuli may be responsible for diminished gastric function. Nevertheless, derangements in efferent signals from the dorsal motor nucleus of the vagus (DMV) to the stomach may also account for reduced motility.

Methods: We assessed the anatomical, neurophysiological and functional integrity of gastric-projecting DMV neurons in T3-SCI rats using: 1) retrograde labeling of gastric-projecting DMV neurons; 2) whole cell recordings from gastric-projecting neurons of the DMV; and, 3) *in vivo* measurements of gastric contractions following unilateral microinjection of thyrotropin releasing hormone (TRH) into the DMV.

Key Results: Immunohistochemical analysis of gastric-projecting DMV neurons demonstrated no difference between control and T3-SCI rats. Whole cell *in vitro* recordings showed no alteration in DMV membrane properties and the neuronal morphology of these same, neurobiotin-labeled, DMV neurons were unchanged after T3-SCI with regard to cell size and dendritic arborization. Central microinjection of TRH induced a significant facilitation of gastric contractions in both control and T3-SCI rats and there were no significant dose-dependent differences between groups.

Conclusions: Our data suggest that the acute, 3 day to 1 week post-SCI, dysfunction of vagally-mediated gastric reflexes do not include derangements in the efferent DMV motoneurons.

Keywords

DMV; Gastroparesis; Neurotrauma; TRH; Vago-vagal reflexes

Spinal cord injury (SCI) imparts immediate, and long-term, changes to motor, sensory and autonomic function. In addition to cardiovascular dysregulation [1-3], gastric dysmotility

Corresponding author: Dr. Gregory M. Holmes, Department of Neural and Behavioral Sciences, Penn State College of Medicine, 500 University Drive, MC H109, Hershey, PA 17033, gmh16@psu.edu.
Author contribution
EMS acquired and analyzed *in vivo* experimental data, performed histological processing, and contributed to writing the manuscript.
GMH designed the study and protocol, acquired and analyzed *in vivo* experimental data, and contributed to writing the manuscript.

occurs following SCI (reviewed in [4]). Specifically, upper gastrointestinal (GI) dysfunction following SCI includes impairment of gastric emptying as well as gastric and intestinal motility.[5-7] Individuals with SCI also present reflux, abdominal pain, bacterial translocation, bloating, and prolonged/delayed colonic transit.[8] One-third of patients with complete quadriplegia for more than 1-year continue to experience GI symptoms.[9] Based upon previous reports, fatalities in SCI patients who initially survived the injury may partially be caused by GI tract complications and depressed immune responses that lead to sepsis.[10-12] In brief, acute failure to regulate GI function following SCI may induce greater morbidity and mortality through eventual bacterial overgrowth and translocation [13,14]

The reflex functions of the upper gastrointestinal organs, most notably the stomach, are modulated by medullary neurons within the dorsal vagal complex (DVC). The DVC is comprised of the area postrema (AP), the nucleus tractus solitarius (NTS), and the dorsal motor nucleus of the vagus (DMV) and is located at the transition from the open to closed medulla. [15] The DVC finely regulates the coordinated delivery of nutrients to the duodenum by integrating GI stimuli that are conveyed through the sensory vagus [16-18], from spinosolitary inputs [19,20], as well as inputs arriving from higher CNS nuclei. [21-23] Furthermore, the DVC has been shown to possess the characteristics of a circumventricular organ [24,25] as well as active transport mechanisms for circulating cytokines. As a result, the DVC is positioned to integrate the presence of circulating factors with neural input. Additionally, passive permeability to blood-borne agents increases following inflammatory and traumatic insults [26] thus rendering the DVC vulnerable to pathophysiological conditions. For example, in animal models of inflammatory bowel disease (IBD), circulating cytokines (IL-1β, IL-6 and TNF-α), presumptively entering the DVC through the permeable blood-brain barrier , initiate an apoptotic cascade resulting in an *in vitro* decrease in DMV proliferation and an *in vivo* decrease in gastric projecting DMV neurons.[27] Furthermore, peripheral injections of IL-1β, systemic activation of TNF- α production, and central administration of TNF-α rapidly suppress gastric motor activity. [28-30] The presence of circulating inflammatory cytokines, including IL-6 and IL-1β have also been reported following experimental and clinical SCI [31,32] and may compromise DMV neuronal function and integrity as part of a larger systemic inflammatory response. [33]

Persistent gastroparesis has been reported in animal models of SCI. [34,35] In particular, we have demonstrated that rats with experimental high thoracic (T3-) SCI show a rapidly-developing, and prolonged, delay in gastric emptying of a [^{13}C]-labeled solid meal. [36] The neurocircuitry comprising the gastric vago-vagal reflex remains anatomically intact after T3-SCI.While our previous report suggests that T3-SCI diminishes vagal afferent sensitivity [37], derangements of gastric efferent signaling may play a role in post-SCI dysmotility that has not been investigated.

The aims of the present study were to use an acute rat model of experimental SCI to investigate 1) if experimental SCI induces rapid degeneration of gastric projecting vagal motoneurons; 2) if the *in vitro* biophysical properties of DMV neurons demonstrate reduced excitability; and 3) if *in vivo* gastric motility continues to respond to brainstem microinjection of thyrotropin releasing hormone (TRH).

Materials and Methods

All procedures followed National Institutes of Health guidelines and were approved by the Institutional Animal Care and Use Committee at the Penn State Hershey College of Medicine. Male Wistar rats ≥8 weeks of age, upon entrance into the experiment, and initially weighing 175-200 g (Harlan, Indianapolis, IN, USA) were used and double housed in a room maintained at 21-24°C and a 12:12-h light-dark cycle with food and water provided *ad libitum*. After surgery animals were single housed, observed daily, and food and body weight were recorded.

Surgical procedures and animal care

Rats were randomly assigned for SCI or surgical control and each group was further divided into 3-day and 1-week post-surgical study groups. Prior to surgery, rats were anesthetized with isoflurane (2-3%, 1 L min^{-1} O_2) as necessary to achieve areflexia (absence of palpebral reflex). All animals were administered ophthalmic ointment to both eyes, buprenorphine (0.01mg kg^{-1}, s.c., Reckitt Benckiser Pharmaceuticals Inc., Richmond VA) to alleviate post-operative pain, and antibiotics (Baytril, 2.5 mg/ml concentration at 1ml kg^{-1} s.c., Bayer, Shawnee Mission KS) to reduce post-surgical infection prior to any surgical manipulation.[36] Once a deep plane of anesthesia was achieved, the skin overlying vertebral thoracic levels 1-3 (T1-T3) was shaved and cleaned with three alternating applications of Nolvasan (Chlorhexidine Acetate, Fort Dodge Animal Health, Fort Dodge, IA) and ethanol. The surgical site was incised 3-4mm along the midline and the underlying spinous processes were cleared of all musculature. Using fine tipped rongeurs, spinal T3 was exposed via laminectomy of the T2 spinous process which extended laterally to the T2 transverse processes as described previously [35,38]. The rats were placed in the Infinite Horizon controlled impact device (Precision Systems and Instrumentation, LLC, Lexington, KY) and clamped via the T1 and T3 spinous processes. Once secure, a rapid 300 kDyne displacement of the cord and overlying dura was performed. Procedures for the control animals were the same as for spinal injury except that the spinal cord and surrounding dura mater was not disturbed following laminectomy. Upon completing the surgical procedure, the muscle tissue overlying the lesion site was closed in anatomical layers with Dexon II suture and the skin closed with 9mm wound clips. Animals were administered warmed supplemental fluids (5 cc lactated Ringer's solution, s.c.) and placed in an incubation chamber maintained at 37° C until the effects of anesthesia had subsided.

Post-operative chronic care of both injured and control animals involved placing corn cob filled animal housing tubs on a warming unit (Gaymar T-pump, Stryker, Kalamazoo, MI) to maintain a warmed environment (ca. 25°C) and received subcutaneous supplemental fluids (5-10 cc lactated Ringer's solution) twice daily, analgesics (buprenorphine 0.01mg kg^{-1}, IP) twice daily for 3 days and antibiotics (Baytril, 2.5 mg kg^{-1}) twice daily for 5 days after surgery. Bladder expression was performed at least twice daily in animals with T3-SCI until the return of spontaneous voiding. The ventrum of control animals was inspected daily without need for manual compression of the bladder. Due to the reduction in locomotor capacity after T3-SCI, a reservoir of chow was placed at head level in order to facilitate ease of access for feeding. All T3-SCI rats ingested a measureable amount each day, thereby

confirming that access to chow was available. Bodyweight and food intake were measured daily for all animals. Since animals were fasted overnight prior to euthanasia, only bodyweight and food intake for day 2 (all animals) and for day 6 (those animals surviving 7-9 days) were selected for analysis. In order to normalize the raw measurements of bodyweight and food intake across animals, mean energy intake (MEI) was calculated by dividing the daily average of kcal consumed per 100 g of bodyweight (bw) for each 2-day period of monitored feeding.

Neuronal tracing

To identify DMV neurons projecting to the stomach, the retrograde neuronal tracer, cholera toxin B subunit (CTB), was injected into the muscular layers of the gastric corpus in one subset of animals (n=18) six days prior to T3-SCI surgery. The rats were anesthetized as above with isoflurane, the abdomen was shaved and prepared for aseptic surgery as described above. The stomach was isolated via an abdominal laparotomy, and CTB (0.5% solution, 5 μl total volume) was injected via a glass micropipette (50 μm diameter) in 4-6 sites so as to encompass a 5 mm^2 region of the anterior gastric corpus following the greater curvature of the stomach. The incision was closed in layers using Dexon II suture and the skin closed with 9mm wound clips. Six days later, wound clips were removed and these animals were randomly assigned to T3-SCI or control surgery. Nine days after T3-SCI or control surgery, rats were euthanized for immunohistochemistry.

Histological Processing

At the conclusion of every experiment, deeply anesthetized rats were transcardially perfused with heparinized phosphate-buffered saline (PBS) until fully exsanguinated and followed immediately with PBS containing 4% paraformaldehyde. The brainstem and spinal cord at the lesion level were removed and refrigerated overnight in PBS containing 20% sucrose and 4% paraformaldehyde. For immunohistochemical processing, the entire rostrocaudal extent of the DVC was sectioned on a freezing stage microtome and alternating coronal slices (40μm thick) were saved in PBS-filled microplate wells for free-floating immunolabeling. For histological staining of brainstem injection sites or T3-SCI lesion extent, tissue was sectioned (40μm thick) and alternating sections were mounted on gelatin coated slides.

To verify lesion severity or control, spinal cord sections were stained with luxol fast blue (LFB) to visualize myelinated fibers. LFB-stained slides were digitally imaged on a Zeiss Axioscope light microscope and Axiocam CCD camera, imported into Adobe Photoshop and contrast digitally enhanced to allow identification and threshold measurements of LFB-stained (i.e., spared) white matter. For individual images, the boundaries of the tissue slice were outlined to determine cross-sectional area. A separate threshold histogram was generated and the pixels corresponding to LFB staining above background were selected. These pixels were quantified and expressed per unit cross-sectional area. [39] The proximity of the T3 lesion center to the cervical enlargement precluded an appropriate determination of spinal cord cross-sectional area in undamaged tissue rostral to the injury (i.e., damaged tissue extended into the cervical enlargement as described in [35]). Therefore, it was necessary that the cross-sectional area of the intact spinal cords at T3 of comparably sized animals be

determined for normalization purposes. LFB-stained myelin in injured tissue was then expressed as a percent of the total spinal cord cross-sectional area as would be predicted by the intact tissue. Based upon our previous report [37] we determined *a priori* that animals with white matter sparing ≤ 25% were categorized as severe injury while those ≥ 25% were categorized as moderate injury.

To verify microinjection sites for *in vivo* recordings, brainstem sections were stained with cresyl violet to verify the placement of the microinjection pipette tip. Stained slides were digitally imaged on a Zeiss Axioscope light microscope, imported into Adobe Photoshop and injection sites were mapped with the aid of a rat stereotaxic atlas. [40]

Immunohistochemistry

After sectioning, free-floating brainstem sections were washed for 30min in a 1:1 pretreatment solution of Triton + PBS (TPBS; 1:200) and hydrogen peroxide. Between each incubation step, sections were rinsed 3×5 minutes in PBS. Sections were blocked for 1 hour in 10% normal donkey serum (NDS) in PBS. Sections were removed from blocking solution and placed directly into primary antibody for incubation at room temperature (Goat α-CTB; List Biologicals, Campbell, CA, USA; 1:40,000 in PBS). Following 48 hours of antibody incubation, sections were removed, washed and then incubated in biotinylated secondary antibody (donkey α goat; 1:500; Jackson ImmunoResearch, West Grove, PA) for 2 hours. The Avidin-Biotin Complex (ABC) Solution (Vectastain Elite ABC kit, Vector Labs, Burlingame, CA) was prepared according to kit directions and sections were incubated for 1 hour. Sections were exposed to a peroxidase reaction (Vector SG SK-4700; Vector Laboratories, Inc. Burlingame, CA 94010) for as long as necessary to reveal immuno-reactive structures (blue CTB-labeled neurons) against a light background. Sections were washed in PBS and mounted onto gelatin-coated glass slides and air-dried overnight. Slides were placed in Clear Rite and coverslipped with Permount. Slides were digitally imaged on a Zeiss Axioscope light microscope and Axiocam CCD camera, imported into Adobe Photoshop for analysis. Cell counts followed a highly-conservative protocol for inclusion. Non-adjacent sections were randomly selected for analysis and only cells with a threshold density in the ≥95th percentile above baseline were counted as immunopositive.

Electrophysiology

Brainstem slices were prepared as described previously.[41,42] Briefly, T3-SCI or control rats (n=5 each) were anesthetized deeply (Isoflurane, 5%, 1 L min^{-1} O_2) and euthanized via administration of a bilateral pneumothorax. The brainstem was removed and cut into 3-4 coronal slices (`300μm thick) encompassing the entire rostro-caudal extent of the DVC. Slices were incubated at 30±1°C in Krebs' solution (in mM: 126 NaCl, 25 $NaHCO_3$, 2.5 KCl, 1.2 $MgCl_2$, 2.4 $CaCl_2$, 1.2 NaH_2PO_4, and 11 dextrose, maintained at pH 7.4 by bubbling with 95% O_2-5% CO_2) for at least 60-90 minutes before use. A single slice was then transferred to a perfusion chamber (volume 500μl) which was placed on the stage of a Nikon E600FN microscope and kept in place with a nylon mesh. Brainstem slices were maintained at 35±1°C by perfusion with warmed Krebs' solution at a rate of 2.5-3.0 ml min^{-1}. DMV neurons were identified by their soma size and location (ventral to the smaller NTS neurons and dorsal to the larger, heavily myelinated hypoglossal neurons). Whole cell

patch clamp recordings were made from DMV neurons using patch pipettes of 2-4MΩ resistance when filled with a potassium gluconate solution (in mM: K gluconate 128, KCl 10, $CaCl_2$ 0.3, $MgCl_2$ 1, Hepes 10, EGTA 1, ATP 2, GTP 0.25 adjusted to pH 7.35 with KOH) and a single-electrode voltage-clamp amplifier (Axopatch 1D, Molecular Devices, Sunnydale, CA). Data were sampled at 10kHz, filtered at 2kHz, digitized via a Digidata 1320 interface and analyzed using pClamp 9 software (Molecular Devices). The liquid junction potential was compensated at the beginning of the experiment; recordings were discarded if the series resistance was >20 MΩ.

Basic membrane properties were assessed as described previously. [43] Briefly, to calculate the membrane input resistance (R_{in}), the instantaneous current displacement was measured after the voltage-clamped membrane was stepped from −50mV to −60mV. To measure the action potential firing characteristics, DMV neurons were current clamped at approximately −60mV and injected with depolarizing current pulses (15ms duration) of intensity sufficient to evoke the firing of a single action potential at the current pulse offset. The action potential duration at threshold was measured, as was the amplitude of the afterhyperpolarization amplitude; the duration of the afterhyperpolarization (decay constant, τ) was fitted to a single exponential equation and measured. To measure the action potential firing frequency, DMV neurons were current clamped at approximately −60mV before being injected with depolarizing current pulses (400ms duration) of increasing intensity (30-270pA). The number of action potentials fired were counted and expressed as pulses per second (p.p.s.).

Morphological reconstructions and analysis

At the end of the electrophysiological recording, Neurobiotin© (2.5%; Vector Laboratories, Burlingame, CA) included in the recording pipette was injected into the neuron via the passage of subthreshold depolarizing current (400ms duration; 0.8Hz for 20min). The neuronal membrane was allowed to reseal for 10-20min following removal of the pipette before the brainstem slice was fixed in Zamboni's fixative (in mM: 1.6% paraformaldehyde, 19mM KH_2PO_4 and 100mM Na_2PO_4 in 240ml saturated picric acid and 1600ml water, adjusted to pH7.4 with NaOH) at 4^0C for at least 24hr.

Brainstem slices were cleared of fixative by repeatedly washing in PBS containing Triton X-100; in mM: 115 NaCl, 75 Na_2HPO_4, 7.5 KH_2PO_4 and 0.15% Triton X-100). Neurobiotin filled neurons were visualized as described previously [41]. Briefly, brainstem slices were incubated with avidin-D- horseradish peroxidase solution (Vector Laboratories; 0.002% avidin D-horseradish peroxidase in PBS containing 1% Triton X-100) for 2hr. The slices were then washed repeatedly in PBS-Triton X before incubation in PBS containing diaminobenzidine, cobalt chloride and nickel sulfate (0.05% diaminobenzidine in PBS containing 0.025% cobalt chloride and 0.02% nickel sulfate) for 30min. Slices were then exposed to 3% H_2O_2 for a period of time sufficient for the adequate visualization of the Neurobiotin-filled neurons. Brainstem slices were mounted on gelatin—subbed slides, air dried and dehydrated through a graded series of alcohols and xylene before being mounted in Permount (Fisher Scientific, Pittsburgh, PA).

The morphological characteristics of Neurobiotin-filled neurons were assessed using Neurolucida software (MBF bioscience, Willison, VT) attached to a Nikon E400 microscope

at a final magnification of X400. Three-dimensional reconstructions of individual neurons were made and morphological properties assessed included soma area, form factor (a measure of soma circularity where 1=perfect circle and 0=straight line), dendritic branching (including number of segments and branch order) and dendritic length in both X- and Y-axes. In order to be accepted, the neuronal reconstruction had to have a mediolateral and rostrocaudal branch extention of at least 200μm with no major branches being severed during the initial sectioning of the brainstem slice and a soma with no obvious damage from pipette retrieval. A subroutine of the Neurolucida software was used to rescale the brainstem slice to 300μm (the thickness of original slicing) to correct for any optical and physical compression that may have occurred during fixation and processing.

Gastric Motility recordings

In vivo gastric motility recordings and intracerebroventricular (ICV) microinjections of TRH in the DVC were performed in control and T3-SCI rats (n=60). Rats, which received only a T3-SCI or control surgery, were randomly divided into 3-day and 1 week post-injury or post-surgical control study groups. Brainstem microinjections of TRH and PBS-control were done in a dose-dependent manner to experimentally test gastric motility. For the following pharmacological experiment, all rats were prepared as follows: Following an overnight fast (water ad libitum), rats were deeply anesthetized with thiobutabarbitol (Inactin®, Sigma; 100–150 mg/kg; IP) and Dexamethasone (1 mg/kg sc, Sigma, St. Louis, MO) was administered to prevent cerebral edema. Rats were then intubated with a tracheal tube to maintain an open airway and a laparotomy was performed. The stomach was isolated and a 6 X 8-mm encapsulated sub-miniature strain gage of our own fabrication was aligned with the circular smooth muscle fibers and sutured to the ventral surface of the gastric corpus. [44] The strain gage leads remained exteriorized before closure of the abdominal incision. After surgical instrumentation, animals were placed in a stereotaxic frame and rectal temperature was monitored and maintained at 37±1°C (TCAT 2LV, Physitemp Instruments, Clifton, NJ). After a midline incision and removal of the overlying dorsal neck musculature, the head of the animal was oriented such that the floor of the fourth ventricle was exposed and the brainstem surface was horizontally oriented in a manner that prevented washout of the solution(s) applied. The pial membrane overlying the vagal trigone was dissected and the exposed tissues were covered with a warm, saline-infused cotton patch. The strain gage signal was amplified (QuantaMetrics EXP CLSG-2, Newton, PA) and recorded on a polygraph (model 79, Grass, Quincy, MA) or on a computer using Experimenter's Workbench software (Datawave Technologies, Loveland, CO). After 1 hour of stabilization, 10 min of baseline motility was recorded before any experimental manipulation. The effects of TRH, (0, 3, or 10 pmoles/60nl) microinjected in the left DVC (at coordinates from calamus scriptorius: +0.1–0.3mm rostro-caudal, 0.1–0.3mm medio-lateral and −0.3-0.5mm dorso-ventral) adjacent to the area postrema, were observed as recorded peaks that increased in frequency, height, and/or rose above baseline [44].

Drugs and chemicals

Inactin® and all other salts were purchased from Sigma (St. Louis, MO). All drugs were dissolved in sterile isotonic phosphate buffered saline (PBS; in mM: 147.6 NaCl, 83.3 NaH_2PO_4, 12.9 KH_2PO_4).

Statistical Analysis

Results are expressed as means ± S.E.M. with significance defined as $P < 0.05$. Between group results from anatomical or *in vivo* studies, between pre- and post-treatment motility values, were compared by one-way ANOVA and Tukey *post hoc* analysis or paired *t*-test as appropriate (SPSS Inc, Chicago, IL). Results from *in vitro* studies were compared using the Student's grouped *t*-test.

RESULTS

Histological assessment of T3-SCI severity

Harvest of the brainstem for *in vitro* electrophysiology precluded processing of the spinal cord for histological analysis. In animals receiving a spinal cord injury for anatomical or *in vivo* studies, the range of total white matter sparing was 2 – 64% of control. Based upon our criteria, animals were categorized as severe injury (range 2 – 24%; n=40) or moderate injury (range 27 – 67%; n=12) and segregated into their respective groups for further behavioral, anatomical and physiological analysis. Due to injury variability and subsequent low sample numbers for the immunohistochemical and motility studies, animals categorized as moderate injury were excluded from further analysis.

Analysis of total white matter of the T3 thoracic spinal cord from control animals that had been prepared for immunohistochemistry or that were tested for motility at 3 days or 1 week after surgery revealed no damage to the spinal cord as a result of the spinal laminectomy (Table 1; $P > 0.05$). Comparisons of control and T3-SCI rats, however, demonstrated a significant reduction of white matter ($P < 0.05$) while there were no group differences between T3-SCI rats prepared for immunohistochemistry or that were tested for motility (Table 1; $P > 0.05$).

Assessment of post-injury weight loss and reduction of spontaneous oral intake of food

There were no significant experimental group differences between the post-operative bodyweights of animals designated as control, nor were there significant experimental group differences between the post-operative bodyweights of animals designated as severe T3-SCI (n = 40, $P > 0.05$). Therefore, the bodyweight and food intake data were collapsed within surgical groups. On the second day after surgery, the bodyweight was significantly lower between T3-SCI and surgical control animals (Table 2; $P < 0.05$). In animals prepared for CTBimmunohistochemistry or tested for gastric motility 1 week after surgery, the mean bodyweight prior to fasting remained significantly lower between T3-SCI and surgical control animals as the bodyweight of surgical controls began to increase while T3-SCI animals remained consistently reduced (Table 2; $P < 0.05$). At this same time point, the MEI displayed significant differences between T3-SCI and surgical control (Table 3; $P < 0.05$). By 1 week, MEI remained significantly reduced in T3-SCI animals compared to surgical controls despite a significant increase from 3 day values in the T3-SCI animals (Table 3; $P < 0.05$). Furthermore, MEI significantly increased from 3 day values for the surgical control animals (Table 3; $P < 0.05$).

Taken together, our histological, bodyweight and feeding data verify the profound severity, effectiveness and reproducibility of our surgical procedures for T3-SCI and surgical control animals. All animals in these groups were selected for further data analysis.

The number of CTB--immunoreactive DMV neurons projecting to the stomach is unaffected by T3-SCI

Labeling of CTB-IR neurons in surgical control and T3-SCI animals revealed corpus-projecting neurons in the DMV projecting to the anterior gastric corpus (Fig. 1). These CTB-IR neurons extended from throughout the caudal, intermediate (sections that included the AP), and rostral DMV. There were no significant differences between T3-SCI and surgical controls in the number of CTB-IR gastric-projecting DMV neurons in the intermediate DMV (control: 34.7±3.4, T3-SCI 39.2±6.7; $P > 0.05$). The intermediate region of the DMV corresponds to our TRH microinjection site. No DMV neurons from T3-SCI neurons displayed signs of necrosis/degeneration (e.g., vacuoles, pyknosis, and/or axonal swelling).

These results suggest that T3-SCI does not induce any overt loss of DMV neurons projecting to the stomach and that the number and staining intensity of parasympathetic preganglionic neurons is similar to surgical controls.

T3-SCI does not alter DMV neuron electrophysiological or morphological properties

Recordings were made from 25 control and 17 T3-SCI neurons. Of these, complete electrophysiological and morphological properties were assessed in 25 and 20 control neurons, respectively, and 13 and 17 T3-SCI neurons, respectively. The membrane properties of DMV neurons from control (n=25 cells) and T3-SCI (n=13 cells) rats were assessed under current clamp or voltage clamp conditions as described previously [43]. As detailed in Table 4, T3-SCI did not affect either the membrane input resistance or action potential firing properties of DMV neurons (Figure 2). Complete morphological properties were assessed in 20 control and 17 T3-SCI DMV neurons and are summarized in Table 5. T3-SCI did not alter any of the morphological features of the recorded DMV neurons (Figure 2).

T3-SCI does not reduce brainstem sensitivity to TRH

Representative raw data traces demonstrate a rapid onset for gastric corpus contractions following microinjection of TRH in all experimental groups (Fig. 3). Histologically verified microinjection of PBS in the left DVC did not induce any significant percent change in gastric motility index above baseline in either control (n = 5) or T3-SCI rats (n = 5; $P > 0.05$; Fig. 4).

In animals tested 3 days after surgery, microinjection of 3 pmol of TRH into the left DVC of control animals induced a significant percent increase in gastric motility index compared to baseline values (n = 5; $P < 0.05$; Fig. 4). Similarly, microinjection of 3 pmol TRH into the left DVC of T3-SCI animals produced a significant percent increase in gastric motility index compared to individual baseline values (n = 5; $P < 0.05$; Fig. 4). Between subjects comparisons revealed there were no significant differences between control (n=5) and T3-

SCI (n=5) animal groups in the percent change of motility index nor the duration of response to 3 pmol TRH ($P > 0.05$; Fig. 4).

In a separate group of animals that were tested 3 days after surgery, microinjection of 10 pmol of TRH into the left DVC of both control and T3-SCI animals induced a significant percent increase in gastric motility index compared to baseline values ($n = 5$/group; $P < 0.05$; Fig. 4). Despite a trend toward an increase from the 3 pmol dose, there was not a significant difference in the percent change in motility index between control animals receiving 3 or 10 pmol TRH ($n = 5$/group; $P < 0.05$; Fig. 4). In addition, there was no significant difference in both the percent change of motility index and response duration to 10 pmol TRH between control and T3-SCI animals (n=5/group; $P > 0.05$; Fig. 4).

A separate cohort of animals was tested 1 week after surgery in order to more closely approximate the post-injury time frame of our animals prepared for histology. Microinjection of 3 pmol of TRH into the left DVC of control animals induced a significant percent increase in gastric motility index compared to baseline values ($n = 5$; $P < 0.05$; Fig. 4). Similarly, microinjection of 3 pmol TRH into the left DVC of T3-SCI animals significantly increased gastric motility index compared to baseline values ($n = 5$; $P < 0.05$; Fig. 4). There was no significant difference in both the percent increase in motility index or response duration to 3 pmol TRH between control and T3-SCI animals (n=5/group; $P > 0.05$; Fig. 4). In a separate group of animals that were tested 1 week after surgery, microinjection of 10 pmol of TRH into the left DVC of both control and T3-SCI animals induced a significant percent increase in gastric motility index compared to baseline values ($n = 5$/group; $P < 0.05$; Fig. 4). The trend toward an increase between the 3 and 10 pmol dose did not reach significance (n=5/group; $P > 0.05$; Fig. 4). In a similar manner, the response duration between control and T3-SCI animals following microinjection of 10 pmol TRH also demonstrated a non-significant trend ($P > 0.05$; Fig. 4).

DISCUSSION

The present study demonstrates that the gastroparesis induced during the acute T3-SCI period does not involve morphological changes of gastric-projecting vagal motoneurons or reduction in motor responses mediated by vagal motoneurons innervating the gastric corpus. Our experimental data indicate that: 1) retrogradely-labeled gastric-projecting DMV neurons demonstrated no difference in the number of CTB-labeled cells between control and T3-SCI rats; 2) whole cell *in vitro* electrophysiological recordings showed similar membrane properties in the DMV of control and T3-SCI rats; 3) the cell size and dendritic arborization of Neurobiotin-labeled DMV neurons were unchanged after T3-SCI; and 4) *in vivo* central microinjection of TRH induced a significant facilitation of gastric contractions in both control and T3-SCI rats with no significant dose-dependent differences between groups. These data suggest that, given the appropriate afferent signals, the vagal efferent limb likely remains fully capable of eliciting gastric motility following T3-SCI and lends further support that diminished vagal afferent input to the brainstem neurocircuitry may be solely responsible for diminished gastric reflexes after T3-SCI[4]. The mechanism leading to this impairment remains to be determined but does not include DMV neuron loss.

Anatomical and physiological changes of DMV neurons have been recently reported within 1 week following perivagal capsaicin[41]. Those studies demonstrated a loss of CTB-labeled, gastric-projecting DMV neurons; decreased input resistance and excitability of DMV neurons as well as a decrease in number of neurons responding to TRH with an increase in action potential firing; and decreased *in vivo* response to brainstem microinjection of TRH. Therefore, we are confident that the similar techniques employed within this study are robust enough to demonstrate any reduction in the efferent limb of vagally-mediated gastric reflexes following SCI.

While perivagal application of a TRPV1 agonist, capsaicin, at a supraphysiological dose (>30mM) does not physiologically reflect endogenous processes resulting in vagal damage [41], emerging evidence in other animal models suggests that vagal afferent and efferent fibers are susceptible to rapid degenerative processes across several disease states. Vagal neuropathies following ischemic insults have been demonstrated within hours following experimental apnea [45] and hypobaric hypoxia [46,47] whereby vagal neuropathy has been proposed as a causal mechanism for cardiac arrhythmias. [48] Vagal neuronal degeneration has also been implicated within hours after the experimental induction of blood-brain barrier dysfunction or trauma [49], diabetes [50,51], and experimentally-induced colitis.[27]

Comorbidities associated with SCI share features with the above pathologies and would, hypothetically, predict DMV degeneration or vago-vagal reflex dysfunction. Specifically, diminished sympathetic tone and reduced cardiovascular reflex function below the level of the lesion may place the GI tract at risk for hypoxia with resulting inflammation. The principal nutritive functions of the GI tract are critically dependent upon adequate blood flow to GI tissues. Not surprisingly, the GI tract is one of the most highly perfused organ systems in the body, and resting GI blood flow is approximately 20-25% of the total cardiac output.[52] Thus, the intestine is one of the most sensitive tissues to hypoxic insult and even brief periods of GI hypoxia induce the production of inflammatory mediators and dysmotility. Furthermore, GI hypoxia may potentially promote oxidative stress associated with inflammation and result in mitochondrial dysfunction within neuronal processes. While our data do not support the hypothesis that acute T3-SCI adversely affects DMV efferent neuronal survival or functional properties, the effects on vagal afferent fibers originating within the GI tract remains to be determined.

Decades of experimental evidence has elucidated the physiological role of TRH (reviewed in [53]) including the vagally-mediated augmentation of gastric contractions. [54-59] Briefly, microinjection of TRH within the dorsal vagal complex (DVC) excites the firing of DMV neurons, thereby stimulating efferent outflow of gastric-projecting vagal neurons. In turn, vagal efferents drive gastric myenteric cholinergic neurons to increase in gastric motility. [60] In fact, thyrotropin releasing hormone (TRH)-containing projections from the medullary raphe serve as an example of how a single agonist can appropriate the function of a vagal gastric control reflex by acting at multiple sites within the reflex circuit.*In vitro* evidence has demonstrated that TRH activates DMV neurons directly by modulating calcium-modulating calcium-dependent potassium conductance. [59] In addition, TRH disinhibits DMV neurons by acting to inhibit neurons in the NTS directly.[61,62] These NTS neurons provide

GABAergic input to the DMV [63] thereby resulting in a net excitation. Finally, TRH potentiates the effects of neurotransmitters that also act to inhibit NTS neurons through the modulation of NTS transduction pathways.[62] The end result is that TRH fully engages medullary gastric reflex control circuitry to produce maximal cholinergic activation of gastric motility. As such, TRH serves as a robust pharmacological tool to study the gastric efferent vagus.

The DVC is regarded as possessing the characteristics of a circumventricular organ.[24,25] Additionally, dendritic arborizations of DMV neurons extend into the area postrema and fourth ventricle. As a result, the DVC is positioned to integrate the presence of circulating factors with neural input.[64,65] Additionally, passive permeability to blood-borne agents increases following inflammatory and traumatic insults[26] thus likely rendering the DVC vulnerable to pathophysiological conditions following SCI. A rapidly-developing systemic inflammatory response has been reported as early as 2 hours following SCI [33] and circulating inflammatory cytokines, including IL-6, IL-1β and TNF-α have been reported following SCI [31,32] that may compromise gastric-projecting DVC neurocircuitry centrally.[28,30] The specific time course of evelvating cytokine levels within the DVC remains obscure and the present study did not monitor circulating levels of inflammatory cytokines following SCI.However, the actions of sub-femtomolar administration of TNF- α within the DVC include a profound and immediate suppression of TRH-stimulated DVC neuronal firing and gastric motility. [30,66] If circulating levels of TNF- α were sufficiently high in the acute phase of T3-SCI, our microinjection experiments with TRH would have been expected to reveal a blunted gastric motility response. While the reported doses of TNF-α [30,66] have been considered to be within the range of circulating levels following systemic infection [67] the interpretation of pro-inflammatory cytokine expression and physiological effects need to be thouroughly addressed in our particular experimental model.

While the post-injury use of prophylactic antibiotic therapy across all groups might affect GI status, previous reports of systemic inflammatory response indicate that prophylactic enrofloxacin (Baytril™) treatment does not appear to influence the cytokine-mediated local and systemic inflammatory response cascade to spinal cord injury. [33] Preliminary data from our own laboratory reveal that local inflammatory responses within GI tissues are detectable despite this standard antibiotic regimen. [68] Our present data suggests that acute cytokine infiltration into the DVC may not be as extensive as what occurred in previous studies, however, this requires further investigation.

Studies on the rate and extent to which normal aging diminishes extrinsic innervation of the GI tract reveal slowly progressing changes to vagal afferent [69] and sympathetic innervation [70], while changes to gastric-projecting vagal neurons remain obscure. Clinically, the progression of SCI-related GI symptoms have been reported to fully develop over a period of several years. [71] Our previous study demonstrated that gastric dysfunction, in the form of diminished gastric emptying of a solid meal and gastric contractions following experimental SCI, developed quickly and persisted over a six week time period. [36] In the present study, we selected time points which overlapped previous demonstrations of DMV pathophysiology.[27,41] One limitation to this approach was the relatively short time course after SCI. Insufficient literature exists with which to determine whether SCI accelerates

aging of the GI tract [72], especially with regard to extrinsic input to the stomach. Premature aging associated with chronic SCI may exert long-term effects on the conductance and overall health of the DMV neurons while peripheral factors play a significant role in adding to the premature degeneration. In a clinical context it is tempting to speculate how the ensuing lack of vagal efferent drive following SCI might ultimately impact the SCI patient. In addition to a well-established modulation of GI function, numerous studies have produced compelling experimental evidence that the DMV is a potent inhibitor of inflammation via what has been coined the cholinergic anti-inflammatory pathway [73]. Briefly, activation of vagal parasympathetic fibers attenuates the systemic inflammatory response to a variety of insults. This effect is mediated via the α7 subunit of the nicotinic acetylcholine receptor, which is expressed on macrophages [74] and other non-neuronal cell types (see [73]). The afferent signaling for this reflex has both neural and humoral components and has received considerable clinical attention.[75] Experimental interruption of this anti-inflammatory reflex, through vagotomy or pharmacological blockade, has a pro-inflammatory effect.[76] Furthermore, indirect vagal activation of the spleen has been shown to be an important component of this reflex.[77,78] Therefore, our observation of diminished vagal efferent signaling to the GI tract may be of particular importance not only to our model of gastric dysfunction following high-thoracic SCI but also contribute to the chronic suppression of immune function.

In conclusion, our data suggest that the gastric dysfunction that immediately accompanies SCI 3 days to 1 week following injury does not include a reduction in the functionality of DMV motoneurons. This observation extends our previous conclusions that dysfunction of gastric vago-vagal reflexes following T3-SCI may be due, in part, to compromised vagal sensory input affecting the gain of vagally-mediated reflexes.[4,37] Clearly, anatomical and functional changes in the integrative neurocircuitry at the level of the NTS remain largely unexplored in acute and chronic animal models of neurotrauma. Understanding the long-term consequences of alterations in vago-vagal neurocircuitry, which remains anatomically intact following SCI, remains crucial for the development of effective therapeutic strategies. Our data identify a potential therapeutic target, the efferent loop of the vago-vagal circuit, for relieving post-SCI gastric dysfunction.

Acknowledgments

Support: NS 49177 (GMH), NS 87834 (EMS). Dr. Kirsteen N. Browning contributed to the *in vitro* study design, data generation and analysis. The authors would also like to express their gratitude to Samuel R. Fortna for his effort assisting with the morphological analysis, Gina Deiter, Kristy Pugh, and Margaret McLean for their assistance in multiple capacities. The authors have no competing interests to disclose.

Funding

This work was supported by National Institutes of Health Grants NINDS 49177 (G.M. Holmes) and NINDS 87834 (E.M. Swartz).

Reference List

1. Weaver LC, Marsh DR, Gris D, Brown A, Dekaban GA. Autonomic dysreflexia after spinal cord injury: central mechanisms and strategies for prevention. Prog Brain Res. 2006; 152:245–63. [PubMed: 16198705]

2. Inskip JA, Ramer LM, Ramer MS, Krassioukov AV. Autonomic assessment of animals with spinal cord injury: tools, techniques and translation. Spinal Cord. Jun 10.2009 47:2–35. [PubMed: 18542091]
3. Krassioukov A. Autonomic function following cervical spinal cord injury. Respir Physiol Neurobiol. Nov 30.2009 169:157–64. [PubMed: 19682607]
4. Holmes GM. Upper gastrointestinal dysmotility after spinal cord injury: Is diminished vagal sensory processing one culprit? Front Physiol. 2012; 3:1–12. [PubMed: 22275902]
5. Wolf C, Meiners TH. Dysphagia in patients with acute cervical spinal cord injury. Spinal Cord. Jun. 2003 41:347–53. [PubMed: 12746741]
6. Kirshblum SC, Groah SL, McKinley WO, Gittler MS, Stiens SA. Spinal cord injury medicine. 1. Etiology, classification, and acute medical management. Arch Phys Med Rehabil. Mar.2002 83:S50–S58. [PubMed: 11973697]
7. Park MI, Camilleri M. Gastroparesis: clinical update. Am J Gastroenterol. May.2006 101:1129–39. [PubMed: 16696789]
8. Fynne L, Worsoe J, Gregersen T, Schlageter V, Laurberg S, Krogh K. Gastric and small intestinal dysfunction in spinal cord injury patients. Acta Neurol Scand. 2012; 125:123–8. [PubMed: 21428967]
9. Lu CL, Montgomery P, Zou X, Orr WC, Chen JD. Gastric myoelectrical activity in patients with cervical spinal cord injury. Am J Gastroenterol. 1998; 93:2391–6. [PubMed: 9860398]
10. DeVivo MJ, Kartus PL, Stover SL, Rutt RD, Fine PR. Cause of death for patients with spinal cord injuries. Arch Intern Med. Aug 1.1989 149:1761–6. [PubMed: 2669663]
11. Miller LS, Staas WE Jr. Herbison GJ. Abdominal problems in patients with spinal cord lesions. Arch Phys Med Rehabil. Sep.1975 56:405–8. [PubMed: 1164181]
12. Riegger T, Conrad S, Schluesener HJ, Kaps HP, Badke A, Baron C, et al. Immune depression syndrome following human spinal cord injury (SCI): A pilot study. Neuroscience. Feb 6.2009 158:1194–9. [PubMed: 18790013]
13. Bohm M, Siwiec RM, Wo JM. Diagnosis and Management of Small Intestinal Bacterial Overgrowth. Nutr Clin Pract. Jun 1.2013 28:289–99. [PubMed: 23614961]
14. Liu J, An H, Jiang D, Huang W, Zou H, Meng C, et al. Study of bacterial translocation from gut after paraplegia caused by spinal cord injury in rats. Spine. Jan 15.2004 29:164–9. [PubMed: 14722407]
15. Browning KN, Travagli RA. Plasticity of vagal brainstem circuits in the control of gastric function. Neurogastroenterol Motil. 2010; 22:1154–63. [PubMed: 20804520]
16. Iggo A. Tension receptors in the stomach and the urinary bladder. J Physiol. Jun 28.1955 128:593–607. [PubMed: 13243351]
17. Blackshaw LA, Grundy D, Scratcherd T. Vagal afferent discharge from gastric mechanoreceptors during contraction and relaxation of the ferret corpus. J Auton Nerv Syst. Jan.1987 18:19–24. [PubMed: 3819312]
18. Raybould, HE. Vagal afferent innervation and the regulation of gastric motor function. In: Ritter, S.; Ritter, RC.; Barnes, CD., editors. Neuroanatomy and physiology of abdominal vagal afferents. CRC Press; Boca Raton: 1992. p. 193-220.
19. Menetrey D, Basbaum AI. Spinal and trigeminal projections to the nucleus of the solitary tract: a possible substrate for somatovisceral and viscerovisceral reflex activation. J Comp Neurol. Jan 15.1987 255:439–50. [PubMed: 3819024]
20. Gamboa-Esteves FO, Tavares I, Almeida A, Batten TF, McWilliam PN, Lima D. Projection sites of superficial and deep spinal dorsal horn cells in the nucleus tractus solitarii of the rat. Brain Res. 2001; 921:195–205. [PubMed: 11720726]
21. Blevins JE, Schwartz MW, Baskin DG. Evidence that paraventricular nucleus oxytocin neurons link hypothalamic leptin action to caudal brain stem nuclei controlling meal size. Am J Physiol Regul Integr Comp Physiol. 2004; 287:R87–R96. [PubMed: 15044184]
22. Morton GJ, Blevins JE, Williams DL, Niswender KD, Gelling RW, Rhodes CJ, et al. Leptin action in the forebrain regulates the hindbrain response to satiety signals. J Clin Invest. Mar.2005 115:703–10. [PubMed: 15711637]

23. Blevins JE, Baskin DG. Hypothalamic-brainstem circuits controlling eating. Forum of Nutrition. 2010; 63:133–40. [PubMed: 19955781]
24. Gross PM, Wall KM, Pang JJ, Shaver SW, Wainman DS. Microvascular specializations promoting rapid interstitial solute dispersion in nucleus tractus solitarius. Am J Physiol Regul Integr Comp Physiol. Dec 1.1990 259:R1131–R1138.
25. Cottrell GT, Ferguson AV. Sensory circumventricular organs: central roles in integrated autonomic regulation. Regul Peptides. Jan 15.2004 117:11–23.
26. Pan, W.; Kastin, AJ. Transport of cytokines and neurotrophins across the blood-brain barrier and their regulation after spinal cord injury. In: Sharma, HS.; Westman, J., editors. Blood-Spinal Cord and Brain Barriers in Health and Disease. Elsevier; 2004. p. 395-407.
27. Ammori JB, Zhang WZ, Li JY, Chai BX, Mulholland MW. Effect of intestinal inflammation on neuronal survival and function in the dorsal motor nucleus of the vagus. Surgery. Aug.2008 144:149–58. [PubMed: 18656620]
28. Tsuchiya Y, Nozu T, Kumei S, Ohhira M, Okumura T. IL-1 Receptor Antagonist Blocks the Lipopolysaccharide-Induced Inhibition of Gastric Motility in Freely Moving Conscious Rats. Dig Dis Sci. 2012; 57:2555–61. [PubMed: 22610882]
29. Hermann GE, Tovar CA, Rogers RC. Induction of endogenous tumor necrosis factor-alpha: suppression of centrally stimulated gastric motility. Am J Physiol. Jan.1999 276:R59–R68. [PubMed: 9887178]
30. Emch GS, Hermann GE, Rogers RC. Tumor necrosis factor-alpha inhibits physiologically identified dorsal motor nucleus neurons in vivo. Brain Res. Oct 4.2002 951:311–5. [PubMed: 12270510]
31. Pan W, Kastin AJ. Increase in TNFalpha transport after SCI is specific for time, region, and type of lesion. Exp Neurol. 2001; 170:357–63. [PubMed: 11476601]
32. Hayes KC, Hull TC, Delaney GA, Potter PJ, Sequeira KA, Campbell K, et al. Elevated serum titers of proinflammatory cytokines and CNS autoantibodies in patients with chronic spinal cord injury. J Neurotrauma. Jun.2002 19:753–61. [PubMed: 12165135]
33. Gris D, Hamilton EF, Weaver LC. The systemic inflammatory response after spinal cord injury damages lungs and kidneys. Experimental Neurology. May.2008 211:259–70. [PubMed: 18384773]
34. Leal PR, Cruz PR, Lopes AC Jr. Lima RC Jr. Carvalho FM, da G Jr. et al. A new model of autonomic dysreflexia induced by gastric distension in the spinal cord-transected rat. Auton Neurosci. Aug 18.2008 141:66–72. [PubMed: 18567543]
35. Tong M, Holmes GM. Gastric dysreflexia after acute experimental spinal cord injury in rats. Neurogastroenterol Motil. 2009; 21:197–206. [PubMed: 19126185]
36. Qualls-Creekmore E, Tong M, Holmes GM. Time-course of recovery of gastric emptying and motility in rats with experimental spinal cord injury. Neurogastroenterol Motil. 2010; 22:62–e28. [PubMed: 19566592]
37. Tong M, Qualls-Creekmore E, Browning KN, Travagli RA, Holmes GM. Experimental spinal cord injury in rats diminishes vagally-mediated gastric responses to cholecystokinin-8s. Neurogastroenterol Motil. 2011; 23:e69–e79. [PubMed: 20950355]
38. Primeaux SD, Tong M, Holmes GM. Effects of chronic spinal cord injury on body weight and body composition in rats fed a standard chow diet. Am J Physiol Regul Integr Comp Physiol. 2007; 293:R1102–R1109. [PubMed: 17634202]
39. Noble LJ, Wrathall JR. Spinal cord contusion in the rat: morphometric analyses of alterations in the spinal cord. Exp Neurol. 1985; 88:135–49. [PubMed: 3979507]
40. Paxinos, G.; Watson, C. Academic Press; New York: 1986. The Rat Brain in Stereotaxic Coordinates.
41. Browning KN, Babic T, Holmes GM, Swartz E, Travagli RA. A critical re-evaluation of the specificity of action of perivagal capsaicin. J Physiol. Mar 15.2013 591:1563–80. [PubMed: 23297311]
42. Swartz EM, Browning KN, Travagli RA, Holmes GM. Ghrelin increases vagally-mediated gastric activity by central sites of action. Neurogastroenterol Motil. 2014; 125:2–22.

43. Browning KN, Renehan WE, Travagli RA. Electrophysiological and morphological heterogeneity of rat dorsal vagal neurones which project to specific areas of the gastrointestinal tract. J Physiol. Jun 1.1999 517:521–32. Pt 2. [PubMed: 10332099]
44. Holmes GM, Swartz EM, McLean MS. Fabrication and implantation of miniature dual-element strain gages for measuring in vivo gastrointestinal contractions in rodents. J Vis Exp. Mar 15.2014 31:1563–80.
45. Zhang JH, Fung SJ, Xi M, Sampogna S, Chase MH. Apnea produces neuronal degeneration in the pons and medulla of guinea pigs. Neurobiol Dis. Oct.2010 40:251–64. [PubMed: 20554036]
46. Luo H, Guo P, Zhou Q. Role of TLR4/NF-kappaB in damage to intestinal mucosa barrier function and bacterial translocation in rats exposed to hypoxia. PLoS One. 2012; 7:e46291. [PubMed: 23082119]
47. Adak A, Maity C, Ghosh K, Mondal K. Alteration of Predominant Gastrointestinal Flora and Oxidative Damage of Large Intestine Under Simulated Hypobaric Hypoxia. Z Gastroenterol. 2014; 52:180–6. [PubMed: 24526402]
48. Aydin MD, Kanat A, Yilmaz A, Cakir M, Emet M, Cakir Z, et al. The role of ischemic neurodegeneration of the nodose ganglia on cardiac arrest after subarachnoid hemorrhage: An experimental study. Experimental Neurology. Jul.2011 230:90–5. [PubMed: 20887724]
49. Wu X, Zhang W, Li JY, Chai BX, Peng J, Wang H, et al. Induction of apoptosis by thrombin in the cultured neurons of dorsal motor nucleus of the vagus. Neurogastroenterol Motil. Mar 1.2011 23:279–e124. [PubMed: 21143557]
50. Tay SS, Wong WC. Short- and long-term effects of streptozotocin-induced diabetes on the dorsal motor nucleus of the vagus nerve in the rat. Acta Anat (Basel). 1994; 150:274–81. [PubMed: 7839795]
51. Yan B, Li L, Harden SW, Epstein PN, Wurster RD, Cheng ZJ. Diabetes induces neural degeneration in nucleus ambiguus (NA) and attenuates heart rate control in OVE26 mice. Exp Neurol. Nov.2009 220:34–43. [PubMed: 19615367]
52. Chou CC. Splanchnic and overall cardiovascular hemodynamics during eating and digestion. Fed Proc. Apr.1983 42:1658–61. [PubMed: 6832382]
53. Tache Y, Yang H, Miampamba M, Martinez V, Yuan PQ. Role of brainstem TRH/TRH-R1 receptors in the vagal gastric cholinergic response to various stimuli including sham-feeding. Autonomic Neuroscience. Apr 30.2006 125:42–52. [PubMed: 16520096]
54. McTigue DM, Rogers RC, Stephens RL Jr. Thyrotropin-releasing hormone analogue and serotonin interact within the dorsal vagal complex to augment gastric acid secretion. Neuroscience Letters. 1992; 144:61–4. [PubMed: 1436715]
55. Hornby PJ, Rossiter CD, Pineo SV, Norman WP, Friedman EK, Benjamin S, et al. TRH: immunocytochemical distribution in vagal nuclei of the cat and physiological effects of microinjection. Am J Physiol. Sep.1989 257:G454–G462. [PubMed: 2506764]
56. Garrick T, Buack S, Veiseh A, Tache Y. Thyrotropin-releasing hormone (TRH) acts centrally to stimulate gastric contractility in rats. Life Sci. Feb 16.1987 40:649–57. [PubMed: 3100898]
57. Krowicki ZK, Hornby PJ. TRH and substance P independently affect gastric motility in nucleus raphe obscurus of the rat. Am J Physiol Gastrointest Liver Physiol. 1994; 266:G870–G877.
58. Gourcerol G, Adelson DW, Million M, Wang L, Tache Y. Modulation of gastric motility by brain-gut peptides using a novel non-invasive miniaturized pressure transducer method in anesthetized rodents. Peptides. Apr.2011 32:737–46. [PubMed: 21262308]
59. Travagli RA, Gillis RA, Vicini S. Effects of thyrotropin-releasing hormone on neurons in rat dorsal motor nucleus of the vagus, in vitro. Am J Physiol. Oct.1992 263:G508–G517. [PubMed: 1329553]
60. Rogers RC, McTigue DM, Hermann GE. Vagal control of digestion: modulation by central neural and peripheral endocrine factors. Neurosci Biobehav Rev. 1996; 20:57–66. [PubMed: 8622830]
61. McCann MJ, Hermann GE, Rogers RC. Thyrotropin-releasing hormone: effects on identified neurons of the dorsal vagal complex. J Auton Nerv Syst. 1989; 26:107–12. [PubMed: 2498419]
62. Browning KN, Travagli RA. The peptide TRH uncovers the presence of presynaptic 5-HT1A receptors via activation of a second messenger pathway in the rat dorsal vagal complex. J Physiol (Lond). 2001; 531:425–35. [PubMed: 11230515]

63. Travagli RA, Gillis RA, Rossiter CD, Vicini S. Glutamate and GABA-mediated synaptic currents in neurons of the rat dorsal motor nucleus of the vagus. Am J Physiol. Mar.1991 260:G531–G536. [PubMed: 1672243]
64. Price CJ, Hoyda TD, Ferguson AV. The Area Postrema: A Brain Monitor and Integrator of Systemic Autonomic State. Neuroscientist. Apr 1.2008 14:182–94. [PubMed: 18079557]
65. Babic T, Browning KN. The role of vagal neurocircuits in the regulation of nausea and vomiting. Eur J Pharmacol. Jan 5.2014 722:38–47. [PubMed: 24184670]
66. Hermann GE, Rogers RC. Tumor necrosis factor-a in the dorsal vagal complex suppresses gastric motility. Neuroimmunomodulation. 1995; 2:74–81. [PubMed: 8521142]
67. Hermann GE, Tovar CA, Rogers RC. LPS-induced suppression of gastric motility relieved by TNFR:Fc construct in dorsal vagal complex. Am J Physiol Gastrointest Liver Physiol. Sep.2002 283:G634–G639. [PubMed: 12181177]
68. Swartz EM, Deiter GM, Holmes GM. Mesenteric hypoperfusion and the induction of inflammation-mediated gastrointestinal dysfunction in rats following experimental spinal cord injury. J Neurotrauma. 2013; 30(15) A11.
69. Phillips RJ, Walter GC, Powley TL. Age-related changes in vagal afferents innervating the gastrointestinal tract. Auton Neurosci. Feb 16.2010 153:90–8. [PubMed: 19665435]
70. Phillips RJ, Powley TL. Innervation of the gastrointestinal tract: patterns of aging. Auton Neurosci. Oct 30.2007 136:1–19. [PubMed: 17537681]
71. Stone JM, Nino-Murcia M, Wolfe VA, Perkash I. Chronic gastrointestinal problems in spinal cord injury patients: A prospective analysis. Am J Gastroenterol. 1990; 85:1114–9. [PubMed: 2389723]
72. Hitzig SL, Eng JJ, Miller WC, Sakakibara BM. An evidence-based review of aging of the body systems following spinal cord injury. Spinal Cord. Jun.2011 49:684–701. [PubMed: 21151191]
73. Pavlov VA, Tracey KJ. The vagus nerve and the inflammatory reflex--linking immunity and metabolism. Nat Rev Endocrinol. Dec.2012 8:743–54. [PubMed: 23169440]
74. Yoshikawa H, Kurokawa M, Ozaki N, Nara K, Atou K, Takada E, et al. Nicotine inhibits the production of proinflammatory mediators in human monocytes by suppression of I-kappaB phosphorylation and nuclear factor-kappaB transcriptional activity through nicotinic acetylcholine receptor alpha7. Clin Exp Immunol. Oct.2006 146:116–23. [PubMed: 16968406]
75. Boeckxstaens, G. The clinical importance of the anti-inflammatory vagovagal reflex. In: Ruud, MBaD, editor. Handbook of Clinical Neurology Autonomic Nervous System. Vol. 117. Elsevier; 2013. p. 119-34.
76. The FO, Cailotto C, van der Vliet J, de Jonge WJ, Bennink RJ, Buijs RM, et al. Central activation of the cholinergic anti-inflammatory pathway reduces surgical inflammation in experimental post-operative ileus. Br J Pharmacol. Jul 1.2011 163:1007–16. [PubMed: 21371006]
77. Cailotto C, Gomez-Pinilla PJ, Costes LM, van d, Di GM, Nemethova A, et al. Neuro-anatomical evidence indicating indirect modulation of macrophages by vagal efferents in the intestine but not in the spleen. PLoS One. 2014; 9:e87785. V. [PubMed: 24489965]
78. Ji H, Rabbi MF, Labis B, Pavlov VA, Tracey KJ, Ghia JE. Central cholinergic activation of a vagus nerve-to-spleen circuit alleviates experimental colitis. Mucosal Immunol. Mar.2014 7:335–47. [PubMed: 23881354]

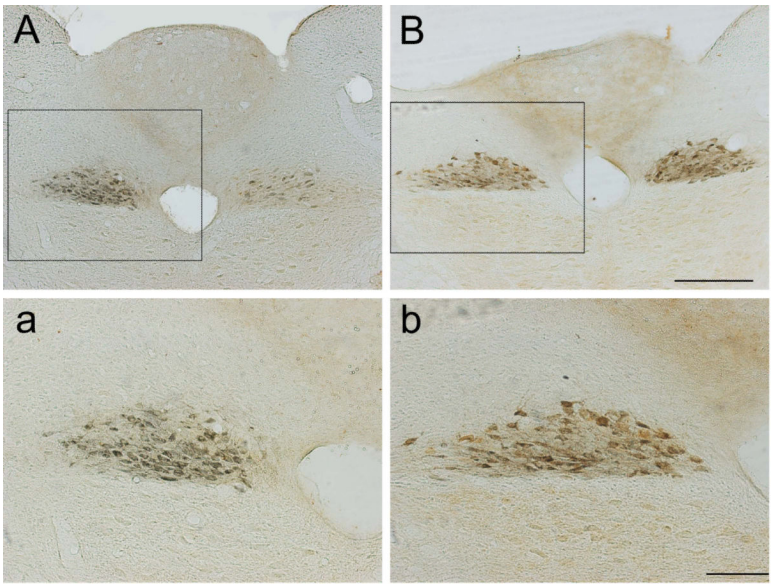

Figure 1. T3-SCI does not induce neuronal degeneration within the dorsal motor nucleus of the vagus (DMV)

Representative low- (10X, A & B) and high- (20X, a & b) power photomicrographs of choleratoxin B-immunopositive dorsal motor nucleus neurons at the level of the area postrema. Region of higher magnification of each corresponding section is indicated within inset. Injection of CTB into the gastric corpus revealed that both control (A, a) and T3-SCI (B, b) rats displayed a comparable number of gastric projecting neurons with no evidence of degeneration. Scale: 500μM in A & B; 50μM in C & D.

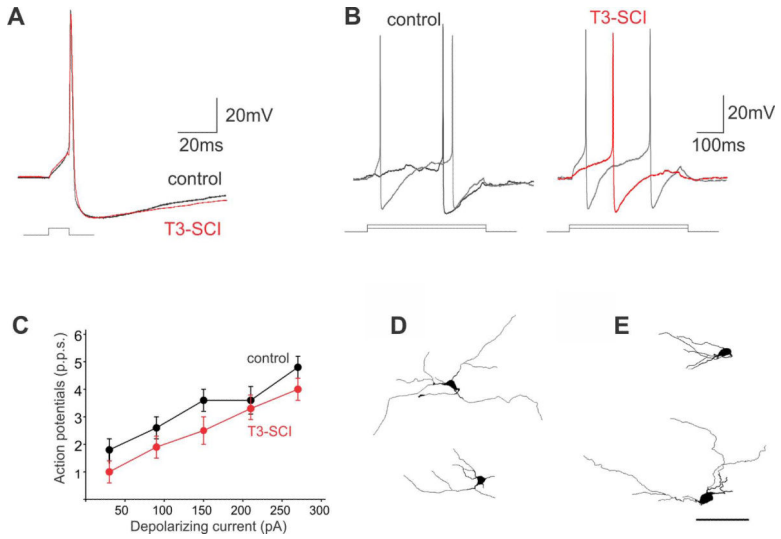

Figure 2. T3-SCI does not alter basic membrane properties or neuronal morphology of DMV neurons

Representative traces illustrating the effects of T3-SCI on action potential properties. (A) DMV neurons were current clamped at −60mV prior to injection of a short (15ms) depolarizing current pulse of intensity sufficient to evoke the firing of a single action potential at current pulse offset. Note that T3-SCI had no effect on action potential duration or afterhyperpolarization amplitude or duration. (B) Control (left) and T3-SCI (right) neurons were current clamped at −60mV prior to injection of long (400ms) depolarizing current pulses of increasing magnitude. Note that the number of action potentials fired was unaffected by T3-SCI. (C) Graphical representation of the frequency of action potential firing (expressed as pulses per second, p.p.s.) in DMV neurons from control (black) and T3-SCI (red) DMV neurons. Note that T3-SCI did not have any significant effect upon the number of action potentials fired in DMV neurons. Representative computer-aided reconstructions of DMV neurons from control (D) and T3-SCI (E) brainstems reveals that T3-SCI did not alter the soma size or dendritic arborization of DMV neurons. Scale: 100μM in A & B.

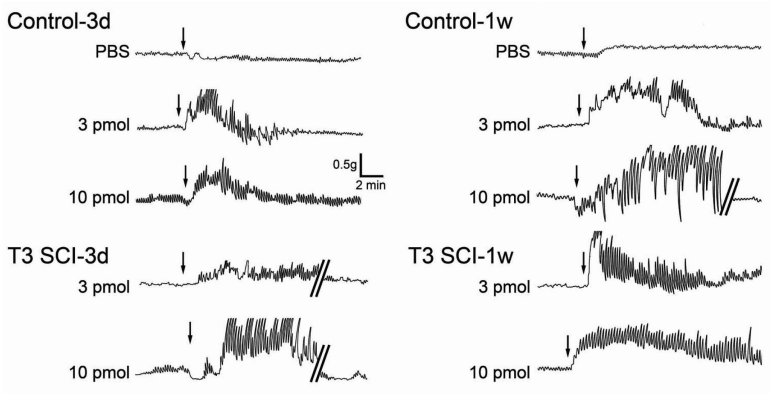

Figure 3. Representative original polygraph traces of gastric corpus contractions from control and T3-SCI

Gastric corpus contractions following microinjection of vehicle (phosphate buffered saline, PBS), 3 pmol or 10 pmol of TRH into the left DVC of animals tested 3 days or 1 week after surgery. Arrows depict the initiation of microinjection for each respective dose. Selected traces are interrupted (denoted by parallel bars) to provide examples of gastric contractions following a return to baseline levels.

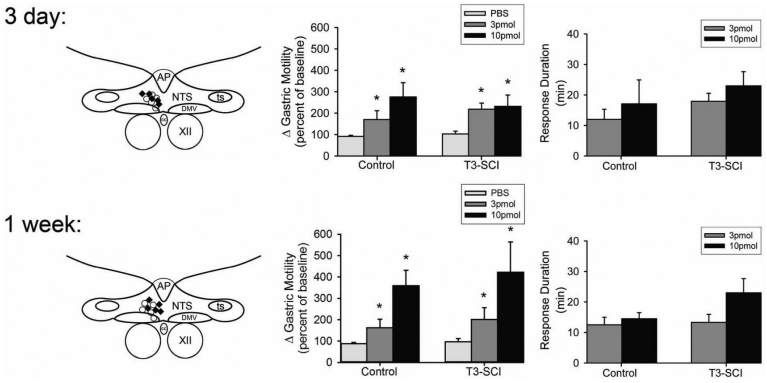

Figure 4. Microinjection of thyrotropin-releasing hormone into the dorsal vagal complex, including the DMV, induces gastric contractions following both control and T3-SCI

Schematic representation of effective injection areas from 3 days (*top left*) and 1 week (*bottom left*) control (marked by ○) or T3-SCI rats (marked by ♦). For clarity, doses of TRH were pooled across surgical treatment groups and only a few examples of the distribution of injection sites are depicted. AP, area postrema; NTS, nucleus tractus solitarius; DMV, dorsal motor nucleus of the vagus; CC, central canal; XII, hypoglossus.

Graphic summary of the increase in gastric corpus motility induced by microinjection of PBS or TRH (3 or 10 pmol, expressed as percent increase from baseline) in the left DVC of 3 day (*top center*) control and T3-SCI (*bottom center*) subjects ($n = 5$ per group; $*p < 0.05$ *vs* pre-microinjection baseline). Duration of the response to microinjection of TRH (*top and bottom right*) was not significantly different between surgical treatment and dose at any time point ($p>0.05$).

Table 1

White matter expressed as a percent of the total spinal cord cross-sectional area.

	Experimental Groups				
	CTB immunohistochemistry	**Motility Studies**			
	1 week post-op	3 day post-op		1 week post-op	
		3pmol TRH	10pmol TRH	3pmol TRH	10pmol TRH
Control	76 ± 1%	77 ± 3%	69 ± 3%	70 ± 2%	70 ± 2%
T3-SCI	15 ± 3%*	8 ± 2%*	14 ± 3%*	14 ± 2%*	7 ± 4%*

*$P<0.05$ vs control

Table 2

Body weight change expressed as percentage of pre-operative weight is reduced following T3-SCI.

	Experimental Groups		
	CTB 6d weight	**3 day post-op 2d weight**	**1 week post-op 6d weight**
Control	102 ± 2%	101 ± 1 %	108 ± 2%
T3-SCI	87 ± 3 %*	91 ± 1 %*	89 ± 3 %*

*$P<0.05$ vs control.

Table 3

T3-SCI decreases normalized food intake (MEI, Kcal/day/100g BW)

	Experimental Groups		
	CTB 6d MEI	**3 day post-op 2d MEI**	**1 week post-op 6d MEI**
Control	24.1 ± 1.1 %	25.8 ± 2.6 %	33.6 ± 3.0 %★
T3-SCI	16.4 ± 3.1 %*	4.9 ± 2.1 %*	25.7 ± 3.1 %*§

*$P<0.05$ vs control,

§$P<0.05$ vs 2d T3-SCI,

★$P<0.05$ vs 2d control.

Table 4

Basic membrane properties of DMV neurons

	Experimental Groups	
	Control (n=20)	**T3 SCI (n=13)**
Input resistance (MΩ)	324±28	336±46
Action potential duration (ms)	2.6±0.1	2.4±0.1
Afterhyperpolarization amplitude (mv)	18.9±0.9	18.8±1.0
Afterhyperpolarization duration (ms)	144±32.6	125±20.3
Action potential firing rate (pps) - 30pA	1.8±0.4	1.0±0.4
Action potential firing rate (pps) - 90pA	2.6±0.4	1.9±0.4
Action potential firing rate (pps) - 150pA	3.6±0.4	2.5±0.5
Action potential firing rate (pps) - 210pA	3.6±0.5	3.3±0.4
Action potential firing rate (pps) - 270pA	4.8±0.4	4.0±0.4

Table 5

Basic morphological properties DMV neurons remain unchanged

	Experimental Groups	
	Control	**T3 SCI**
	(n=20)	**(n=17)**
X-axis	333±39	332±41
Y-axis	190±26	233±46
Soma area	223±12	227±16
Soma diameter	23±1.0	22±0.7
Form factor	0.5±0.07	0.6±0.67
Segment length	210±23	213±18